HYGROTHERMAL ANALYSIS OF HYBRID ELECTRICALLY CONDUCTIVE ADHESIVE AT OPTIMAL MICRO-NANO FILLERS RATIO

Z. Adnan[1], S.H.S.M. Fadzullah[1*], G. Omar[1], Z. Mustafa[2], and B. Çoşut[3]

[1]Faculty of Mechanical Technology and Engineering (FTKM),,
Universiti Teknikal Malaysia Melaka, Hang Tuah Jaya,
76100 Durian Tunggal, Melaka, Malaysia.

[2]Faculty of Industrial and Manufacturing Technology and Engineering (FTKIP),
Universiti Teknikal Malaysia Melaka, Hang Tuah Jaya,
76100 Durian Tunggal, Melaka, Malaysia.

[3]Department of Chemistry,
Gebze Technical University (GTU),
41400, Gebze,Kocaeli,Türkiye.

*Corresponding Author's Email: hajar@utem.edu.my

ABSTRACT: Recent advancements have significantly advanced hybrid electrically conductive adhesive (HECA) as a pivotal polymer-based interconnector in electronic packaging. However, the durability of these materials remains uncertain, particularly under severe thermal and humid conditions, where current literature provides limited explanation. This paper evaluates the reliability of epoxy-based HECA formulations by varying micro-nano ratios of silver micro-flakes and multiwalled carbon nanotubes (AgMF-MWCNT), ranging from 0.07 to 0.27. The study subjects these formulations to hygrothermal exposure at 85°C and 85% relative humidity over a 3 week ageing period. The evaluation employs gravimetric measurement for water absorption, four-point probe testing for electrical conductivity, lap shear testing for mechanical strength, and scanning electron microscopy (SEM) for morphological analysis. Results show the most favorable ratios are 0.07 and 0.17, which achieve the best electrical and mechanical properties respectively.

Upon hygrothermal ageing, anomalous behavior was found in water absorption as weight loss occurs after the first week of ageing. SEM reveals that cracks, delamination, filler pull-out, and filler-matrix debonding were observed on the fractured surface of HECA. In summary, the HECA formulation with a 0.17 ratio demonstrates optimal reliability across all evaluated parameters, underscoring its potential for robust electronic packaging applications.

KEYWORDS: *hybrid ECA; hygrothermal; electronic materials; failure analysis; micro-nano*

1.0 INTRODUCTION

The performance of electrically conductive adhesive (ECA) as an eco-friendly interconnecting agent is potentially deteriorated by electromagnetic interference (EMI) between electronic devices, showing the need for both reliable conductivity and shielding characteristics of the ECA. In light of this issue, epoxy is the best polymer-based composite among other contemporary materials in its category. Carbon is the most suitable material other than metal and metal oxides commonly used to provide EMI shielding ability [1]. Furthermore, to ensure good functionality while maintaining an environmentally friendly product, hybrid ECA (HECA) is the material of choice due to better performance obtained via combined intrinsic properties involving two or more conductive fillers [2–4], compared to normal (non-hybrid) ECA.

Specifically, geometrical factors like shape and size are crucial in enhancing the electrical properties of HECA besides the type of incorporated conductive fillers [5,6]. For example, silver (Ag) as a conductive filler has been well known for excellent electrical conductivity but often puts a major drawback in mechanical and adhesion properties of ECA [7], along with a high intrinsic percolation threshold ranging between 60 to 80 wt.% [8,9]. In light of this issue, E. dal Lago et al. (2020), in their comparative study among multiwalled carbon nanotube (MWCNT), graphene (GR), and carbon black (CB) in single filler ECA, reported the lowest electrical percolation threshold value recorded by MWCNT with 10 nm diameter and >150 aspect ratio, followed by GR and CB [10]. More interestingly, in the literature, numerous researchers discovered a significant improvement in functional properties through hybridization between micro-nano fillers at an appropriate ratio [11,12].

From another perspective, a reliable HECA must demonstrate significant longevity. Excellent functional performance in a typical environment may significantly deteriorate under elevated temperatures and relative humidity (RH) over an extended exposure period, described as hygrothermal ageing. For example, Shetty et al. (2020), in their study on carbon fibre-reinforced epoxy, reported that a higher exposed temperature (70°C) induced more significant deterioration in both tensile and compression strengths due to a higher percentage of moisture absorption, plus reaching moisture equilibrium faster than at a low temperature (45°C) [13]. Besides that, the amount of moisture absorption, which may have been facilitated by polymer swelling, was found responsible for the degradation of adhesive and mechanical interlocking on the adhesion interface [14]. Furthermore, the moisture attack lowered the density of the cross-linked chain in the epoxy, thus simultaneously lowering the glass transition temperature of ECA [15]. Moreover, a mass loss may also occur in the event of polymer chain breaking and carbon-carbon/carbon-hydrogen bond dissociation when subjected to ultraviolet radiation (UV) [16].

Nonetheless, those stated findings were primarily conducted in fibre-reinforced epoxy composite, as too limited studies in the literature evaluated the reliability of HECA, showing a dire need for a further investigation regarding this matter. A HECA study demonstrated an appropriate ratio of micro-silver flakes and boron nitride (AgMF-BN) HECA gradually increases the reliability performance in terms of contact resistance and lap shear strength simultaneously, despite an approximately equivalent rate of moisture absorption with normal ECA [17]. More recently, Nasaruddin et al. (2019) revealed that at a saturated filler loading regarding percolation threshold occurrence, the higher electrical conductivity of MWCNT-filled ECA upon hygrothermal effect was higher achieved for both high and low MWCNT aspect ratios [18]. The increasing amount of filler loading contributes to reducing moisture content [19], while the amount of moisture absorbed is responsible for the deterioration of electrical durability attributed to epoxy degradation [20].

Hence, the present work reports on HECA reliability at optimal range with varying AgMF-MWCNT hybrid fillers ratio at a constant 5 wt.% total filler loading indicated as a critical filler concentration (percolation threshold) in the past research [18]. In this developed HECA, targeting the percolation threshold is the utmost significant correlation that satisfies both electrical and mechanical abilities. Our

previous work had revealed a constant decrement of mechanical integrity beyond the percolation threshold, although at an optimum hybrid fillers ratio [21]. Thus, the role of AgMF-MWCNT optimal ratio in enhancing the reliability of HECA was further evaluated to provide a better insight towards improving the durability of HECA under hygrothermal ageing.

2.0   METHODOLOGY

2.1   Raw Materials

The polymer matrix employed in the present HECA was a two-component epoxy, consisting of diglycidyl ether bisphenol-A (DGEBA) epoxy resin or commercially known as Araldite® M from Sigma Aldrich, coupled with D-230 Polyether amine as a curing agent obtained from JEFFAMINE Huntsman Singapore Pte Ltd. The epoxy and curing agent were stated with the density of 1.168 gcm^{-3} and 0.948 gcm^{-3} at 20°C, respectively. The conductive filler component of HECA involved a micro-nano hybridization using a high aspect ratio MWCNT with an average size of 15 nm diameter and 20 μm length as stated by the manufacturer, Nanostructured & Amorphous Materials Inc. (NanoAmor). The MWCNT has >95% purity and a density of 2.1 gcm^{-3}. The micro-filler used was AgMF supplied by Sigma Aldrich with 99% purity and 10.49 gcm^{-3} density, consisting of 10 μm average flakes size. The intrinsic electrical resistivity of MWCNT and AgMF were <0.01 Ω.cm and 1.59 μΩ.cm, respectively.

2.2   Sample Formulation and Preparation

In this work, the total filler loading was set at 5 wt.%. In addition, the percolation threshold of MWCNT-filled ECA was reported [18] since the significant amount of filler in this HECA system was incorporated by MWCNT. At the beginning of the experimental stage, different micro-nano ratios were considered with an increasing relative amount of AgMF from 0.07 to 0.47, while the total filler was kept constant. This approach has been found to play a critical role in ensuring an optimum performance of HECA involving hybrid fillers with different intrinsic percolation threshold values [21]. Moreover, mechanical strength deteriorated beyond the threshold limit due to the filler agglomeration phenomenon. Therefore, in the next stage (hygrothermal ageing), an optimal range of micro-nano ratios was chosen based on the electrical and mechanical properties for further assessment of reliability study.

Table 1 specified the formulation of HECA in this work.

Table 1: Formulation of HECA

Polymer Matrix (wt.%)		Hybrid Fillers (wt.%)		Micro-nano Ratio	Total hybrid fillers	
Epoxy	Hardener	AgMF	MWCNT		wt.%	vol.%
71.97	23.03	0.35	4.65	0.07	5	2.55
		0.85	4.15	0.17		2.34
		1.35	3.65	0.27		2.13
		1.85	3.15	0.37		1.91
		2.35	2.65	0.47		1.70

The epoxy-hardener stoichiometric mixing ratio was controlled at 100:32 as practiced in the literature [22–26], whereby this ratio provides an optimum characteristic covering all terms including glass transition, flexibility, impact, tensile, compressive, shear, and peel strengths [27]. Therefore, the relative weight percentage (wt.%) was calculated using a 75.76:24.24 epoxy-hardener absolute ratio applied to the 95 wt.% polymer matrix part.

Initially, the epoxy was pre-mixed with AgMF and MWCNT for 2 minutes using the Thinky Mixer ARE-310 centrifugal mixer prior to weighing each material via ME204E Mettler Toledo analytical balance before loading. The hardener was then added, followed by 5 minutes of final mixing to obtain a uniform dispersion. Finally, the HECA suspension was fabricated for different tests before being completely cured inside a Memmert oven UF55 model at 130°C for 3 hours. Four sample batches were made for each formulation, divided into the first batch as reference data (without ageing), followed by the second to fourth batch for 1, 2, and 3 weeks of hygrothermal ageing. After the conditioning process, all characterization tests were conducted by stage (upon unloading the samples) under room temperature and humidity at 26±1°C and 60±5% RH.

2.3 Hygrothermal Conditioning and Moisture Absorption Analysis

Throughout all hygrothermal ageing periods, the moisture absorption of HECA was analyzed as per ASTM D5229 [28]. Samples were initially oven-dried under 70°C [29] until reaching moisture equilibrium after 9 hours for initial weight via gravimetric measurement. This data

collection can be done either before or after the conditioning process. The samples were then conditioned at elevated temperature and relative humidity (RH) of 85°C and 85% RH in a Memmert Humidity Chamber HCP 108 model. Prior to conditioning, the samples were taken out periodically starting from 168 h (1 week), followed by 336 h (2 weeks) and 504 h (3 weeks) to be tested following each type of characterization.

Upon unloading, the samples' surfaces were immediately wiped with a dry cloth, weighed to an accuracy of 0.1 mg on the analytical balance before being tested. The moisture absorption analysis was performed using equation (1):

$$M\ (\%) = \frac{W_t - W_i}{W_t} \times 100 \tag{1}$$

where M is moisture content (%), while W_t and W_i are data at a time and initial (oven-dry) of the sample's weight (g). The data on moisture absorption, volume resistivity, and lap shear strength for each week was obtained after an entire ageing period.

2.4   Electrical Characterization

Employing a four-point probe test, a glass slide was used as an insulating substrate to withstand high temperatures while curing the HECA. The sample preparation and testing were conducted as per ASTM F390 [30]. With explicitly controlled strip's length, width, and thickness of 12 x 3 x 0.1 mm, the fabricated HECA was characterized via In-Line Four-Point Probe coupled with a Jandel RM3000+ Test Unit as shown in Figure 1. This method measures the electrical resistance of the specimen by supplying current via both outer probes. At an instant, another two inner probes measure the voltage drops to provide an exact measurement.
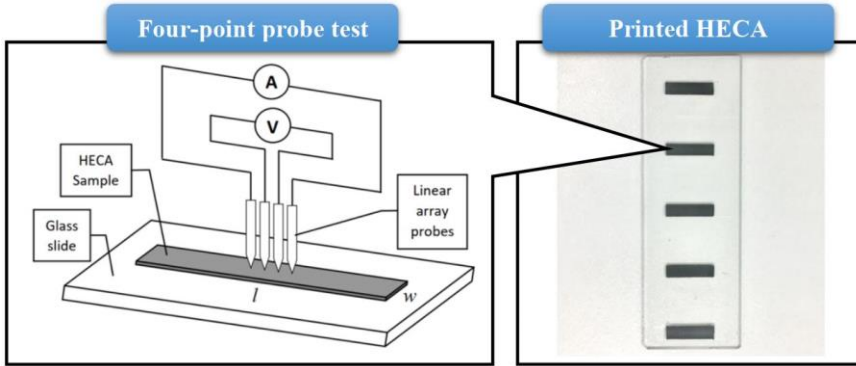
Figure 1: Four-point probe electrical test on printed HECA

A total of five identical strips were considered to represent the average data for each sample. From this test, the volume resistivity of HECA was calculated using an expression given in equation (2):

$$\rho = \frac{V}{I} G t_s \tag{2}$$

where ρ is volume resistivity (Ω.cm), V is supplied voltage (V), I is the current supplied (A), G is correction factor (constant value of 2.7005), and t_s is sample's thickness (cm). The dimension of the sample determines the value of the correction factor according to the stated reference standard, which relies on length-to-width (l/w) and width-to-probe spacing (w/s) ratios.

2.5   Mechanical Characterization

In the lap shear test sample preparation, 1.6 mm thick aluminium sheets were chosen due to high thermal and mechanical durability, as per ASTM D1002 [31]. These metal sheets were cut to specific dimensions using a shearing machine to prevent distortion or bending, especially at the cutting edges by manual cutting that could introduce variation in results. The lap shear sample consists of a coupling substrate assigned with overlap and grip areas, as illustrated in Figure 2. The overlap area referred to as the test area was set to 322.58 mm² whereas the grip area refers to both end parts clamped onto the tensile fixture during force applied.
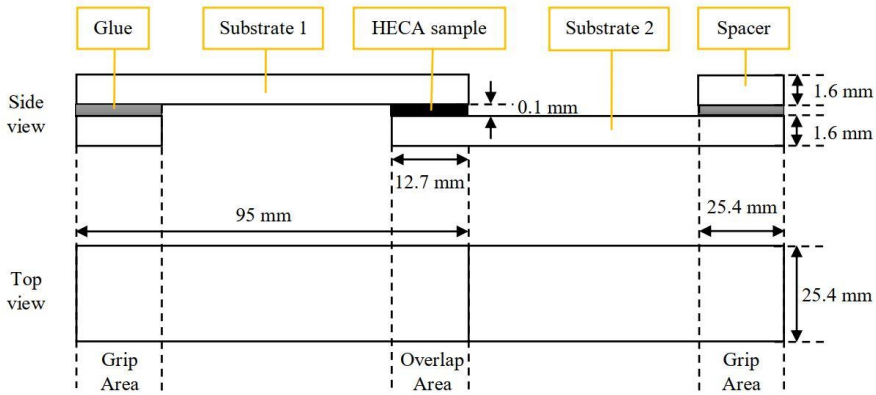
Figure 2: Detailed schematic drawing of HECA sample preparation for lap shear test

The samples preparation was made with reference to Zheng et al. (2021) [32], by attaching the coupling substrates using a custom-designed jig shown in Figure 3 to align the overlapping joint between the coupling substrates and to control the thickness of the HECA sample as well as the limit of the overlap area. Furthermore, to ensure a parallel shear force act on the HECA during tensile loading along with a proper gripping when set up on the fixture of Universal Testing Machine (UTM), an equivalent thickness of square aluminium sheet with dimension given in the schematic diagram was used as a spacer located at the grip area of the sample [33].
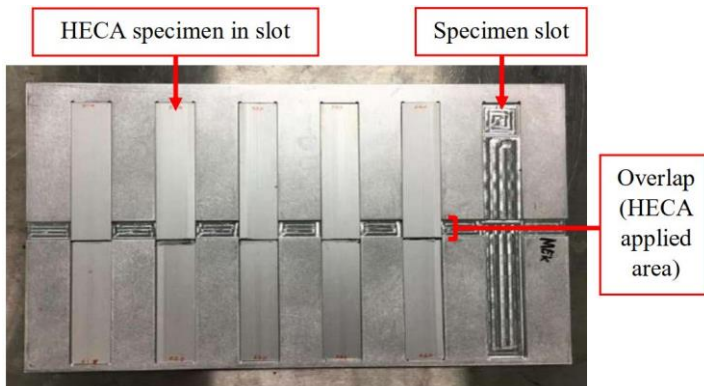

Figure 3: Lap shear test samples prepared on a custom-designed jig before curing

This quasi-static test was conducted on a test-to-failure basis, with a 1.3 mm/min crosshead displacement rate to examine the maximum load

until fracture. Five samples were measured for one formulation in obtaining reliable average data. The lap shear strength of HECA was calculated using an expression given in equation (3):

$$\sigma_{lap} = \frac{F_{max}}{A_{overlap}} \tag{3}$$

where σ_{lap} is the lap shear strength (MPa), F_{max} is the maximum force during failure (N), and $A_{overlap}$ is the area of overlap joint (mm^2). The fractured samples were further characterized in a morphological study through visual and SEM analysis in the post-lap shear test.

2.6   Morphological Characterization

Selected HECA samples were examined in the morphological study using Scanning Electron Microscope (SEM), JEOL JSM-6010PLUS/LV model with an accelerated voltage of 20 kV. A cross-sectional approach was employed for reliable analysis regarding cracks and delamination on adhesive-substrate bonding interface [34]. Nonetheless, surface morphology was more effective for analysis on fractured samples. Before being analyzed, the HECA samples were prepared on the sample stage and sputter-coated with platinum for 4 minutes to inhibit charge for enhanced visualization. In addition, the content of the hybrid filler was confirmed via Energy Dispersive X-Ray (EDX) analysis prior to SEM characterization.

3.0   RESULTS AND DISCUSSION

3.1   Functional Properties of HECA by Varying Micro-nano Ratio

As demonstrated in our previous work, one total filler loading owns considerable uncertainty in terms of electrical conductivity under different ratios between hybrid fillers, thus making it the most crucial factor to be heeded on [35]. Specifically, a highly connected electrical networking is achieved through efficient filler-filler contacts, while the nano-fillers (MWCNT) facilitate electrons transportation within larger micro-fillers (AgMF) with their unique 1-D geometry. Figure 4 (a) visualized the variation of electrical performance in HECA as a function of the micro-nano ratio. The trend recorded the lowest

resistance at the lowest ratio with 6.835±0.385 Ω.cm, suggesting nanofillers most efficient dispersion within the micron-sized AgMF, thus maximizing the formation of electrically conductive paths [36].
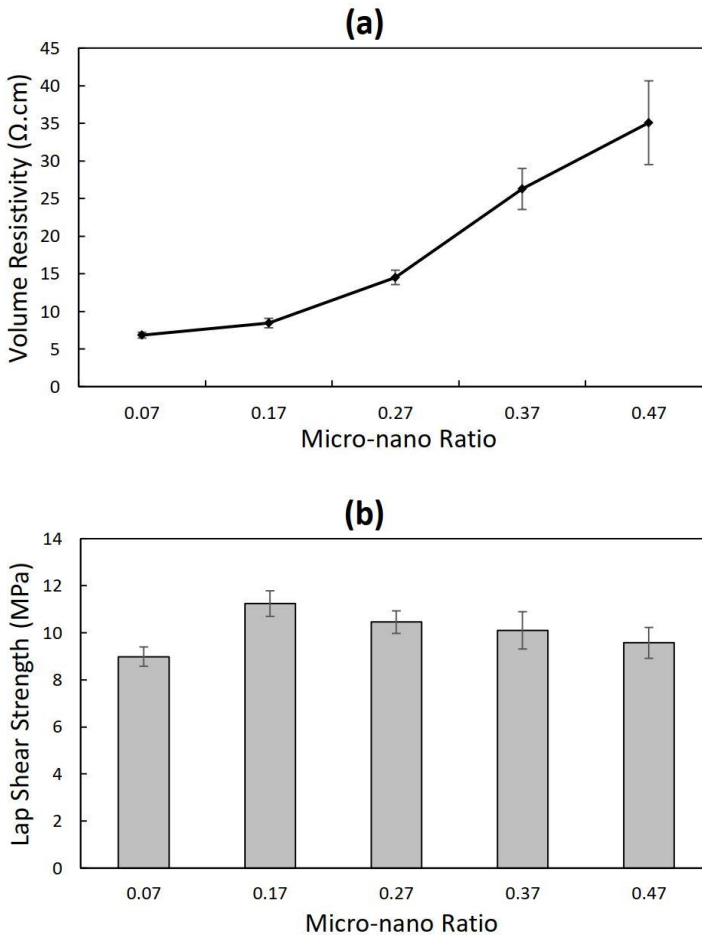
(a)

(b)

Figure 4: Effect of Varying Micro-nano Ratio on; (a) Volume Resistivity and (b) Lap Shear Strength of HECA

However, further increasing ratio to 0.47 gradually reduced the volume resistivity as much as 413.22% from the initial value, which agrees with the previous work regarding hybridization using micro-nano filler that observed deterioration in electrical performance even worse than non-hybrid ECA when a high micro-nano ratio was adopted [37]. In essence, in their research on micro-nano Ag fillers, Ma et al. (2018) found that the nano-sized branches on silver dendrites created vast electrons networking within AgMF particles, thus improving the

electrical performance [5]. In this context, the higher amount of AgMF as in increasing ratios attempted simultaneously to lessen the MWCNT as the relative filler, reducing the bridging component in the hybrid system. Such explanation is imperative of aggressive data inclination towards the higher ratios, which sit at 23.58%, 112.39%, and 284.41% for 0.17, 0.27, and 0.37 ratios, respectively. In volume fraction (vol.%), MWCNT holds a significant contribution than AgMF towards total vol.% of both fillers due to approximately 5 times smaller intrinsic density. Hence, the highest amount of MWCNT owns the highest total filler vol.%, resulting in more electrical networks. This criterion clearly explains the decrease in HECA electrical performance from 0.07 to 0.47 AgMF-MWCNT ratio since the total filler loading in the hybrid system decreases from 2.55 vol.% to 1.7 vol.%.

In a mechanical context, the effect of the micro-nano ratio on the lap shear strength of HECA is highlighted in Figure 4 (b). Unlike in the electrical part, a non-continuous trend is revealed starting with increasing lap shear strength to the highest 11.24±0.544 MPa at 0.17 ratio, due to a 25.07% improvement from the previous ratio. One-dimensional CNT combined with a high aspect ratio is crucial in obtaining efficient interfacial bonds, thus promising results [38,39]. Plus, Luo et al. (2016) stated that the enhancement of tensile strength could be achieved via a high magnitude of contacts between polymer chains and Ag flakes at an appropriate amount [40]. At this point, it is possible that in terms of mechanical integrity, the best formulation of HECA is discovered, which utilizes the advantages of each constituent filler while overcoming their intrinsic deficiency when incorporated together [3].

However, the lap shear strength decreases from the highest value as much as 7.0% at the 0.27 ratio and then continues with a constant decrease towards the 0.47 ratio. This condition is similar to HECA's strength behaviour beyond the mechanical percolation threshold. Since these ratios were monitored in a constant total filler, the deterioration in strength is associated with the addition of AgMF and reduction of MWCNT content, as an overloaded crosslinking along with bridging points due to incorporation of Ag particles are a non-favorable phenomenon that replaces the primary binder connection with metal-

metal interaction [41]. Plus, the amount of MWCNT as the reinforcing agent was minimized along with the increasing micro-nano ratio; thus, the stress distribution upon load exertion becomes less efficient than the optimum 0.17 ratio. Considering both electrical and mechanical terms explained on HECA's functionality, the optimal range was chosen between 0.07 to 0.27 ratios for the hygrothermal ageing test. The reason is that 0.07 and 0.17 ratios represent the highest electrical and mechanical performance. In contrast, the 0.27 ratio owns acceptable functionality, which would provide valuable data for firming the focused finding in monitoring the effect of optimal micro-nano ratio on the reliability of HECA.

3.2 Water Absorption Behaviour of HECA by Varying Micro-nano Ratio

Moisture absorption in HECA is primarily driven by the hydrophilic properties of epoxy and the gaps or voids formed by the inclusion of AgMF. However, via micro-nano hybridization, the infiltration of water molecules is partially overcome as some of the nano-fillers occupy those gaps, thus reducing the diffusion rate into the epoxy [17]. Figure 5 presents the water absorption behaviour of HECA with different micro-nano ratios in the whole ageing period. The observed trend shows that the water absorption rate decreases with an increasing relative amount of AgMF, thus indicating that the gaps/voids are less severe due to the filling effect of MWCNT.
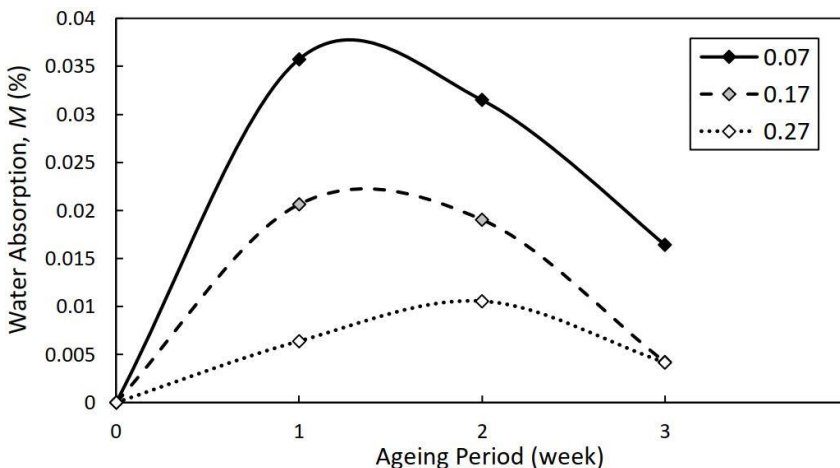

Figure 5: Plot of moisture absorption in HECA subjected to hygrothermal

ageing

Comparing all ratios in the first week, 0.07 ratio in which having richest MWCNT content absorbed moisture the most, followed by 0.17 and 0.27. In this regard, the effect of MWCNT is imperative, as the hollow structure combined with open-end structural characteristics owned was believed to allow water molecules diffused through the MWCNT itself. Corresponding to this issue, the sheet-like shape of GNP, which is similar to AgMF used in this study, was claimed to provide a more efficient barrier towards moisture diffusion, increasing tortuosity and resulting in the lowest permeability when compared to MWCNT [42]. Therefore, the moisture diffusion level is directly proportional to incorporated MWCNT [43,44]. This condition proves that the decrement of moisture absorption is more significant than the increment level, attributed to the decreasing amount of MWCNT to diffuse water molecules and the formation of voids associated with incorporating AgMF. Furthermore, it is why at the 0.27 ratio, the moisture absorption (%) occurs the least, while the 0.17 ratio recorded a moderate level.

In contrast with normal moisture diffusion behaviour, following the first week of ageing, the HECA experienced considerable weight loss, except for the 0.27 ratio, which experienced weight loss after the second week. In this regard, cracks and micro-voids in-between fillers stores moisture, thus promoting weight gain (as found in the first week). However, epoxy's peeling and dissolution occurred at the non-interlocked area by fillers imposed by extended high-temperature exposure causing weight reduction as reported in the literature [45]. As this phenomenon controls the significant weight loss, the net decrease in the overall sample's weight is observed until the end of the ageing period. Moreover, it can be implied that AgMF is a good water barrier. Here, a delay of weight loss observed for the 0.27 ratio is strongly related to the lowest overall amount of diffused water, resulting in slower progress in reaching saturation level in HECA upon humid and thermal conditioning.

Further discussion regarding the weight loss phenomenon upon moisture attack on epoxy had been circulating on chain-breaking

among epoxy molecular structures caused by hydrolysis, which is argued as a vital cause on this issue [46]. It was reported that at 410°C of the hydrolysis reaction, the coupling DGEBA epoxy resin and polyamine hardener is 100% degraded by liquefaction [47]. Although epoxy weight loss is mainly attributed to the desorption process, it also occurs during absorption. The rate of chain scission increases swiftly with increasing chemical reaction with water until to a certain extent where the molecular chains are cut into more than two. Thus, the separate segments are leached subsequently [48]. Hence, this phenomenon is imperative regarding the weight loss of HECA upon reaching the final week of exposure in high temperature and humidity conditions.

3.3 HECA Fracture and Failure Mechanism under Hygrothermal Effect

Characterization of fracture morphology via SEM analysis
The main factor of adhesive fracture is epoxy cracking. Specifically, those crack propagations that occur at epoxy-filler boundaries are initiated by stress and strain localization, induced by irregular volumetric expansion when moisture is absorbed into epoxy [46]. In light of this issue, the interface stress concentration is overcome by excellent stiffness of MWCNT, resulting in a good adhesion found at the optimum 0.17 ratio in Figure 6 (a), whereby the HECA failed cohesively, as clearly evident via 2000 magnification. Besides that, cracks are found on the fractured surface of HECA depicted in Figure 6 (b), most likely due to plasticization and swelling of the matrix that degrades its mechanical integrity. Still, a reliable adhesion is shown by epoxy debris at fracture [49].
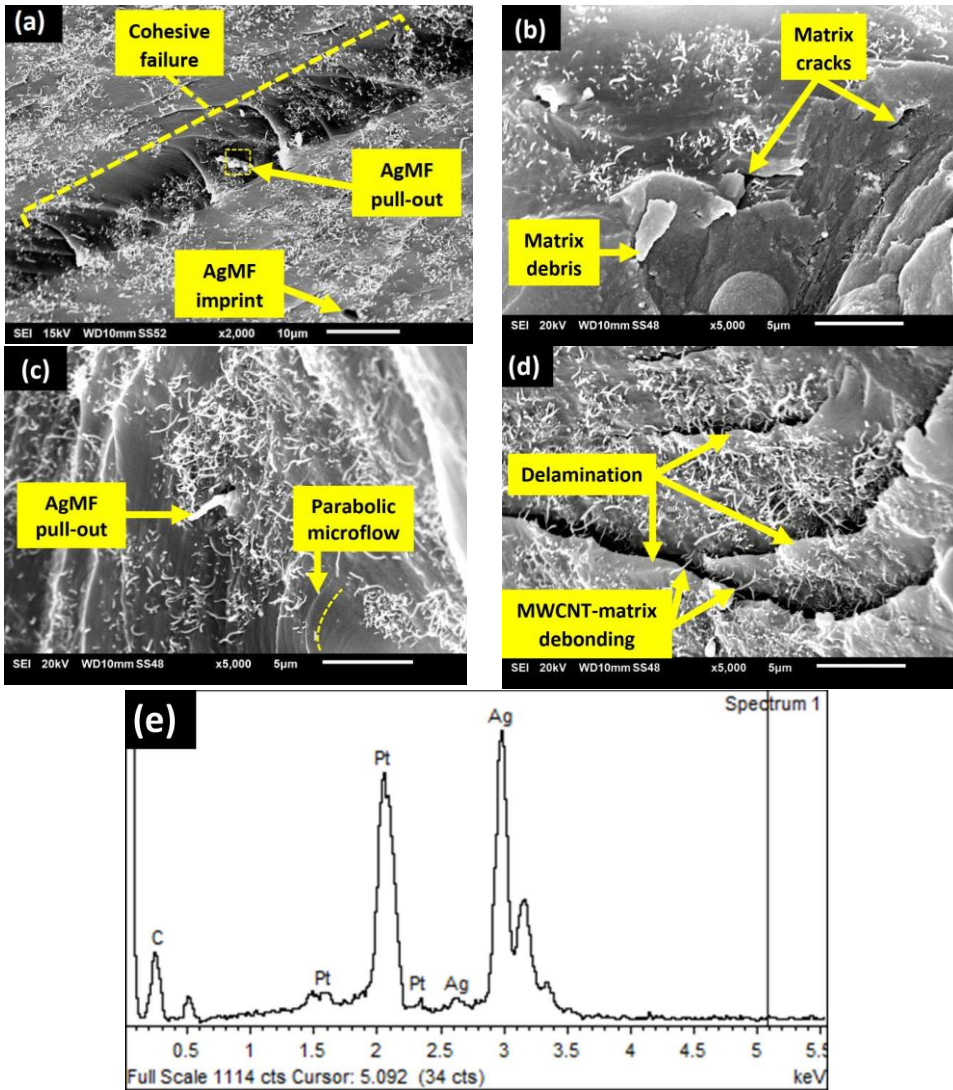
Figure 6: SEM images of the fractured surface of HECA after 3 weeks of hygrothermal ageing for; (a) and (b) 0.17 ratio; (c) and (d) 0.07 ratio; (e) EDX spectrum on the fracture surface of HECA

For 0.07 ratio, it is evident in Figure 6 (c) that a parabolic microflow occurred upon fracture, which implies non-homogenous filler distribution of HECA. It may be associated with saturated MWCNT content that is more challenging in ensuring a completely uniform dispersion without inciting agglomeration. This type of microflow is

formed due to a secondary fracture that is locally inconsistent with the primary fracture's direction, thus finally creating a boundary in the parabolic form [50]. Besides that, AgMF pull-out is observed with poor interfacial bonding with the matrix. Under hygrothermal exposure, the absorbed moisture promoted by high temperature had worsened the crack occurrence.

Other factors, such as delamination and debonding, are evident in Figure 6 (d), thus lowering the tensile strength [13]. At higher AgMF filler loading, another study found that creep deformation becomes severe due to weaker epoxy-AgMF wrapping effect under prolonged hygrothermal ageing [51]. In a composite, the filler-epoxy interface is the most critical factor determining durability. Too high and too low filler-epoxy interfacial bonding strength will induce brittle failure and ease of delamination occurrence, respectively [52]. Hence, the delamination revealed that the interfacial bonding between the matrix with hybridized AgMF-MWCNT had been compromised after hygrothermal exposure. Further confirmation was made by an EDX spectrum given in Figure 6 (e), which was performed on the fractured surface (yellow square mark in Figure 9 (a)), showing the presence of AgMF and MWCNT at the dissociation area with relative atomic content of 58.35%, 29.62%, and 12.03% for Carbon (C), Silver (Ag), and Platinum coating (Pt) respectively.

Ultimately, the role of optimum combination of AgMF and MWCNT at 0.17 ratio is affirmative due to maximized 2-D surface contact of Ag flakes and high aspect ratio MWCNT with polymer matrix, which is the most favorable criteria for an efficient water barrier as shown in the in a comparative illustration in Figure 7. At this instant, the main criteria for both functional properties are highlighted, as the electrical conductivity only needs filler-filler interactions to provide adequate performance. Still, in a mechanical context, filler-matrix interaction is also very crucial. Hence, an electrically optimized (at 0.07 ratio) particles distribution in a hybrid system does not always ensure a reliable strength. Still, when the structure of composite is mechanically optimized (at 0.17 ratio), which is achieved by filler-filler and filler-matrix efficiency. That is why the 0.17 ratio HECA performs well in the overall tests after the hygrothermal ageing, although the highest

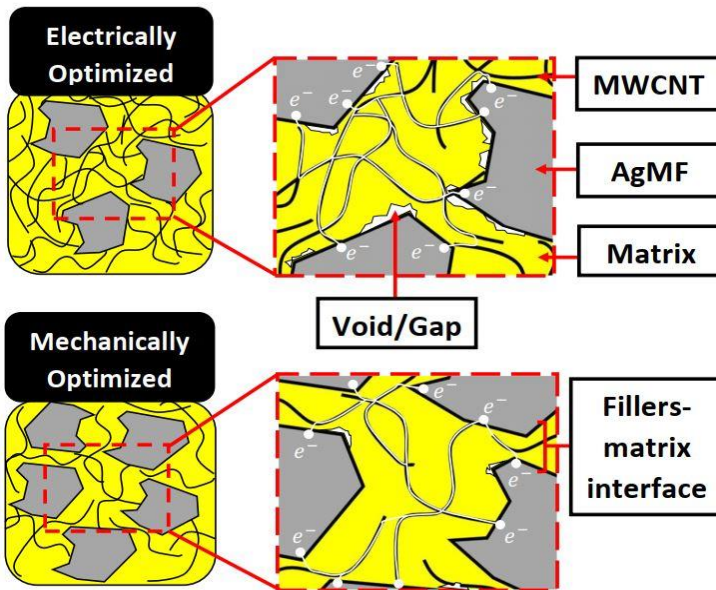performance in electrical property was initially marked at the 0.07 ratio.

Figure 7: Illustration of HECA's structural property on electrically and mechanically optimized particle distribution

For the 0.27 ratio, as shown in Figure 8, the SEM analysis reveals resin-rich sites on the fractured surface, which has little to no participation of hybrid fillers. It suggests the lowest optimality of the micro-nano ratio due to the reduction of MWCNT content as the significant filler in the hybrid system. From Figure 11 (a), the formation of river lines indicates a brittle adhesion that usually fails before the failure of the overall composite, thus cannot represent the overall strength of HECA. The resin-rich site, which often occurs during composite fabrication with low filler loading, has to be minimized by ensuring uniform mixing. This issue contributes to brittleness and other matrix defects such as cracks and voids due to non-optimal curing [53].
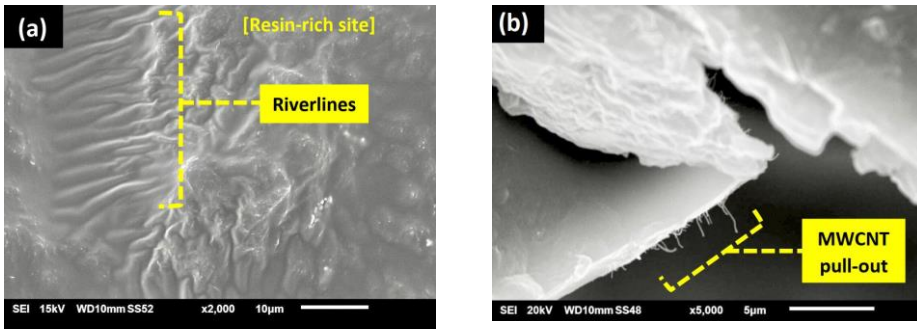
Figure 8: SEM images of the fractured surface of HECA with 0.27 micro-nano ratio at; (a) resin-rich sites; (b) MWCNT pull-out area
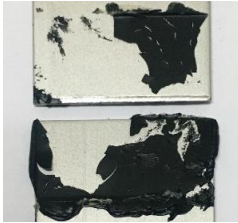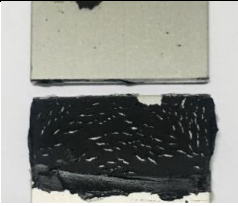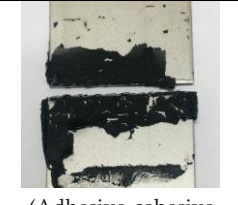
Nevertheless, MWCNT pull-out is revealed in Figure 11 (b), which is believed to be the strengthening element in HECA that aids the strength level at this ratio due to excellent wettability in the matrix. In addition, the high surface area of one-dimensional MWCNT maximizes epoxy-filler 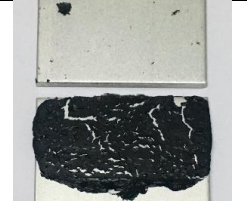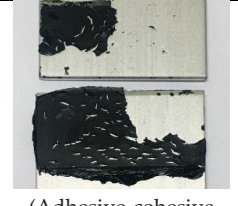interfacial bonding, thus providing good adhesion durability under applied humid and thermal ageing. In this regard, another study demonstrated that MWCNT is vital in enhancing and maintaining the interfacial shear strength between carbon fibre (filler) and epoxy and providing pull-out and bridging effect, thus hindering the associated micro-crack propagation with the hygrothermal impact [54].

The mode of failure is essential considering the adhesion behaviour of HECA, which is given in Table 2. It is important to note that the coupling agent at the interface plays a vital role in determining the adhesion behaviour, load, and stress transfer via the coupling chain at the adhesive-substrate interface [15][52]. Since the amount of epoxy-hardener part is kept constant in this HECA study, the role of the micro-nano ratio is clearly distinguished in determining adhesion behaviour associated with reliability performance.

Nonetheless, all HECA samples tested after the first week resulted in adhesive failure. Polymer degradation is believed to be responsible in this regard, referring to the first phase of the hygrothermal effect as discussed in the previous section. Therefore, the negative impact towards adhesion shows that the mechanical interlocking by penetration into the surface irregularity was lacking at this stage. Thus,

substrate surface roughness needs to be increased to allow more surface area [55]. At this level, the change in the mechanism of failure mode suggests ductile/brittle transition due to deleterious moisture attack on epoxy crosslinking that causes chains to break and segments leach [15]. Another study on the shear failure mechanism of single lap joint also found an agreement with this case, in which they specifically described as the adhesive failure main occurs at the corner (corner failures) indicate the temperature and humidity factors mainly affect the four edges on the bonding area [32].

Table 2: Failure modes of single-joint lap shear samples along ageing period

Week	Micro-nano Ratio		
	0.07	0.17	0.27
0	(Adhesive failure)	(Adhesive-cohesive failure)	(Adhesive-cohesive failure)
1	(Adhesive failure)	(Adhesive failure)	(Adhesive failure)
2	(Adhesive failure)	(Adhesive-cohesive failure)	(Adhesive-cohesive failure)
3	(Adhesive failure)	(Adhesive-cohesive failure)	(Adhesive-cohesive failure)

An exciting part of these data is that upon reaching the second week, the adhesion failure of 0.17 and 0.27 ratios tends to mark a good adhesion behaviour as an adhesive-cohesive failure was seen. The second phase of the hygrothermal effect is imperative regarding this finding, whereby epoxy improved the barrier from moisture attack in the occurrence of post-curing effect [56]. Another researcher explained another description of the side failure pattern. It happened that the adhesive failure rarely occurs at the center of the bonding area, which demonstrated a significant adhesion ability under hygrothermal ageing [32]. Still, the corner of the bonding area seems affected due to the initial stage of degradation effect, resulting in adhesive failure at these areas.

In the final week, similar findings are observed for all micro-nano ratios varied in HECA. The lowest 0.07 ratio exhibited adhesive failure, while an adhesive-cohesive failure was found for HECA with 0.17 and 0.27 ratios. This qualitative finding demonstrated an excellent adhesion performed at the initial condition, resulting in covalent scission on the adhesive instead of the adhesive-substrate interface. However, the adhesive failure behaviour was found for HECA with the lowest 0.07 ratio, due to lower bonding strength than the force exerted during tensile loading.

4.0   CONCLUSION

From the reliability analysis conducted on HECA in this study, several conclusions can be drawn:

i.   The micro-nano hybridization incites anomalous behaviour of moisture absorption in which higher water barrier effect observed through increasing MWCNT-AgMF ratio.

ii.   Morphological analysis verifies the effect of hygrothermal ageing on the HECA sample where cracks, delamination, filler pull-out, and filler-matrix debonding can be detrimental towards the durability of HECA's adhesion strength.

iii.   Moreover, failure mode analysis provides a good indication along the hygrothermal ageing period in which the adhesion

strength of HECA with 0.17 and 0.27 ratios were slightly restored during the second week, shown by the partial cohesive failure.

iv. The outcome in this study reveals an optimum micro-nano ratio at 0.17 ratio, which satisfies all attributes tested. However, the 0.07 ratio offers slightly better performance in electrical performance. Furthermore, it is evident that both AgMF and MWCNT have a trade-off contribution on strengthening and weakening impact on HECA durability; thus, optimal formulation employed in this study ultimately proven a successful enhancement compared to non-hybrid ECA in the past studies.

ACKNOWLEDGMENTS

AUTHOR CONTRIBUTIONS

Z. Adnan: Data Curation and original draft manuscript preparation; S.H.S.M. Fadzullah: Supervision, validation, writing-reviewing and final editing, G. Omar: Co-Supervision and Validation; Z. Mustafa: Optimization of the adhesive formulation, B. Çoşut: Validation and Input on the manuscript write-up

CONFLICTS OF INTEREST

The manuscript has not been published elsewhere and is not under consideration by other journals. All authors have approved the review, agree with its submission and declare no conflict of interest on the manuscript.

REFERENCES

[1]   P. Banerjee and Y. Bhattacharjee, "Lightweight epoxy-based

composites for EMI shielding applications," *Journal of Electronic Materials*, vol. 49, pp. 1702–1720, 2020.

[2] B. M. Amoli, A. Hu, N. Y. Zhou, and B. Zhao, "Recent progresses on hybrid micro-nano filler systems for electrically conductive adhesives (ECAs) applications," *Journal of Materials Science: Materials in Electronics*, vol. 26, pp. 4730–4745, 2015.

[3] M. Oleksy, K. Szwarc-Rzepka, M. Heneczkowski, R. Oliwa, and T. Jesionowski, "Epoxy resin composite based on functional hybrid fillers," *Materials*, vol. 7, no. 8, pp. 6064–6091, 2014.

[4] F. Marcq, P. Demont, P. Monfraix, A. Peigney, Ch. Laurena, T. Falat, F. Courtade, and T. Jamin, "Carbon nanotubes and silver flakes filled epoxy resin for new hybrid conductive adhesives," *Microelectronic Reliability*, vol. 51, no. 7, pp. 1230–1234, 2011.

[5] H. Ma, Z. Li, X. Tian, S. Yan, Z. Li, X. Guo, Y. Ma, and L. Ma, "Silver flakes and silver dendrites for hybrid electrically conductive adhesives with enhanced conductivity," *Journal of Electronic Materials*, vol. 47, no. 5, pp. 2929–2939, 2018.

[6] C. P. Wong, R. Zhang, and J. C. Agar, "Conductive polymer composites," *The Encyclopedia of Polymer Science and Technology*, pp. 1–43, 2011.

[7] Q. Wang, S. Zhang, G. Liu, T. Lin, and P. He, "The mixture of silver nanowires and nanosilver-coated copper micron flakes for electrically conductive adhesives to achieve high electrical conductivity with low percolation threshold," *Journal of Alloys and Compounds*, vol. 820, pp. 1–11, 2020.

[8] J. Zhu, H. Jin, M. Zhou, and X. Zhang, "Electrical property of electrically conductive adhesives filled with micro-sized Ag flakes and modified by dicarboxylic acids," in *17th International Conference on Electronic Packaging Technology (ICEPT 2017)*, China, 2016, pp. 923–926.

[9] W. Qiao, H. Bao, X. Li, S. Jin, and Z. Gu, "Research on electrical conductive adhesives filled with mixed filler," *International Journal of Adhesion and Adhesives*, vol. 48, pp. 159–163, 2014.

[10] E. dal Lago, E. Cagnin, C. Boaretti, M. Roso, A. Lorenzetti, and M. Modesti, "Influence of different carbon-based fillers on electrical and mechanical properties of a PC/ABS blend," *Polymers*, vol. 12, no. 1, pp. 1–16, 2020.

[11] G. Suriati, M. Mariatti, and A. Azizan, "Effects of filler shape and size on the properties of silver-filled epoxy composite for electronic applications," *Journal of Materials Science: Materials in Electronics*, vol. 22, no. 1, pp. 56–63, 2011.

[12] J. Wen, Y. Tian, C. Hang, Z. Zheng, H. Zhang, and Z. Mei, "Fabrication of novel printable electrically conductive adhesives (ECAs) with excellent conductivity and stability enhanced by the addition of polyaniline nanoparticles," *Nanomaterials*, vol. 9, no. 960, pp. 1–10, 2019.

[13] K. Shetty, R. Bojja, and S. Srihari, "Effect of hygrothermal aging on the mechanical properties of IMA/M21E aircraft-grade CFRP composite," *Advanced Composites Letters*, vol. 29, pp. 1–9, 2020.

[14] F. M. G. Ramíreza, F. P. Garpelli, R. de C. M. Sales, G. M. Cândido, M.

A. Arbelo, M. Y. Shiino, M. V. Donadona, "Hygrothermal effects on the fatigue delamination growth onset in interlayer toughened CFRP joints," *International Journal of Fatigue*, vol. 138, pp. 1–12, 2020.

[15] Y. C. Lin, X. Chen, H. J. Zhang, and Z. P. Wang, "Effects of hygrothermal aging on epoxy-based anisotropic conductive film," *Materials Letters*, vol. 60,no.24, pp. 2958–2963, 2006.

[16] Y. Xu, Y. Fang, K. Wang, W. Liu, and H. Fang, "Improving durability of glass fiber reinforced polymer composites by incorporation of ZnO/OMMT nanoparticles subjected to UV radiation and hygrothermal aging," *Materials Research Express*, vol. 7, no. 3, pp. 1–15, 2020.

[17] H. W. Cui, D. S. Li, Q. Fan, and H. X. Lai, "Electrical and mechanical properties of electrically conductive adhesives from epoxy, micro-silver flakes, and nano-hexagonal boron nitride particles after humid and thermal aging," *International Journal of Adhesion and Adhesives*, vol. 44, pp. 232–236, 2013.

[18] M. M. Nasaruddin, *Reliability performance of epoxy based electrically conductive adhesive with varying multiwalled carbon nanotube*, MSc Thesis, Universiti Teknikal Malaysia Melaka, 2019.

[19] R. Keshavarz, H. Aghamohammadi, and R. Eslami-Farsani, "The effect of graphene nanoplatelets on the flexural properties of fiber metal laminates under marine environmental conditions," International *Journal of Adhesion and Adhesives*, vol. 103, pp. 1–11, 2020.

[20] S. Wang, D. S. Pang, and D. D. L. Chung, "Hygrothermal stability of electrical contacts made from silver and graphite electrically conductive pastes," *Journal of Electronic Materials*, vol. 36, no. 1, pp. 65–74, 2007.

[21] Z. Adnan, S. H. S. M. Fadzullah, G. Omar, Z. Mustafa, M. B. Ramli, N. Razali, and A. A. Kamarolzaman, "Hybrid electrically conductive adhesive (HECA) properties as a function of hybrid filler ratio with increasing total filler loading," *Electronic Materials Letters*, vol. 17, pp. 369–383, 2021.

[22] Z. A. Ghaleb, M. Mariatti, Z. M. Ariff, and J. Ervina, "Preparation and properties of amine functionalized graphene filled epoxy thin film nano composites for electrically conductive adhesive," *Journal of Materials Science: Materials in Electronics*, vol. 29, no. 4, pp. 3160–3169, 2018.

[23] C. L. Poh, M. Mariatti, M. N. Ahmad Fauzi, O. Sidek, T. P. Chuah, and S. C. Chow, "Dielectric and thermal properties of treated and untreated MWCNT filled DER 332 epoxy and OP392 epoxy," *Procedia Chemistry*, vol. 19, pp. 865–870, 2016.

[24] G. Suriati, M. Mariatti, and A. Azizan, "Silver-filled epoxy composites: Effect of hybrid and silane treatment on thermal properties," *Polymer Bulletin*, vol. 70, pp. 311–323, 2012.

[25] S. K. Anuar, M. Mariatti, A. Azizan, N. C. Mang, and W. T. Tham, "Effect of different types of silver and epoxy systems on the properties of silver/epoxy conductive adhesives," *Journal of Materials Science: Materials in Electronics*, vol. 22, no. 7, pp. 757–764, 2011.

[26] K. L. Chan, M. Mariatti, Z. Lockman, and L. C. Sim, "Effects of the size and filler loading on the properties of copper- and silver-nanoparticle-filled epoxy composites," *Journal of Applied Polymer Science*, vol. 121, no.6, pp. 3145–3152, 2011.

[27] B. Burton, D. Alexander, H. Klein, A. Garibay-Vasquez, A. Pekarik, and C. Henkee, *Epoxy formulations using JEFFAMINE® polyetheramines*, Huntsman Corporation, pp. 1–103, 2005.

[28] American Society for Testing and Materials, *ASTM D5229*, pp. 1–18, 2014.

[29] K. Majerski, B. Surowska, and J. Bienias, "The comparison of effects of hygrothermal conditioning on mechanical properties of fibre metal laminates and fibre reinforced polymers," *Composites Part B*, vol. 142, pp. 108–116, 2018.

[30] American Society for Testing and Materials, ASTM F390-98, pp. 1–4, 2003.

[31] American Society for Testing and Materials, ASTM D1002, pp. 1–6, 2010.

[32] G. Zheng, Z. He, K. Wang, X. Liu, Q. Luo, Q. Li, and G. Sun, "On failure mechanisms in CFRP/Al adhesive joints after hygrothermal aging degradation followed by mechanical tests," *Thin-Walled Structures*, vol. 158, pp. 1–12, 2020.

[33] N. Masaebi, S. Jamaleddin, and P. Iraj, "Electrically conductive nanocomposite adhesives based on epoxy resin filled with silver-coated nanocarbon black," J*ournal of Materials Science: Materials in Electronics*, vol. 29, no. 14, pp. 11840–11851, 2018.

[34] H. W. Cui and W. H. Du, "Novel fast-curing electrically conductive adhesives from a functional epoxy and micro silver flakes: Preparation, characterization, and humid-thermal aging," *Journal of Adhesion*, vol. 89, no. 9, pp. 714–726, 2013.

[35] S. H. S. M. Fadzullah, Z. Adnan, G. Omar, Z. Mustafa, N. A. B. Masripan, M. R. Mansor, and M. A. Salim, "Effect of hybridization on the functional properties of AgMF–MWCNT-filled electrically conductive adhesive," *Journal of Electronic Materials*, vol. 49, pp. 6572–6581, 2020.

[36] Y. H. Ji, Y. Liu, G. W. Huang, X. J. Shen, H. M. Xiao, and S. Y. Fu, "Ternary Ag/epoxy adhesive with excellent overall performance," *ACS Applied Materials & Interfaces*, vol. 7, no. 15, pp. 8041–8052, 2015.

[37] M. Liang and K. L. Wong, "Electrical performance of epoxy resin filled with micro particles and nanoparticles," in *1st International Conference on Energy and Power*, Energy Procedia, vol. 110, pp. 162–167, Australia, 2017.

[38] H. Xu, J. Al-Ghalith, and T. Dumitrică, "Smooth sliding and superlubricity in the nanofriction of collapsed carbon nanotubes," *Carbon*, vol. 134, pp. 531–535, 2018.

[39] T. H. Nam, K. Goto, Y. Yamaguchi, E. V. A. Premala, Y. Shimamura, Y. Inoue, K. Naito, and S. Ogihara, "Effects of CNT diameter on mechanical properties of aligned CNT sheets and composites," *Composites Part A: Applied Science and Manufacturing*, vol. 76, pp. 289–

298, 2015.

[40] J. Luo, C. Li, M. Chen, and Q. Li, "Electrically conductive adhesives based on thermoplastic polyurethane filled with silver flakes and carbon nanotubes," *Composites Science and Technology*, vol. 129, pp. 191–197, 2016.

[41] H. W. Cui, J. T. Jiu, K. Suganuma, and H. Uchida, "Super flexible, highly conductive electrical compositor hybridized from polyvinyl alcohol and silver nano wires," *RSC Advances*, vol. 5, no. 10, pp. 7200–7207, 2015.

[42] P. Jojibabu, G. D. J. Ram, A. P. Deshpande, and S. Rao, "Effect of carbon nano-filler addition on the degradation of epoxy adhesive joints subjected to hygrothermal aging," *Polymer Degradation and Stability*, vol. 140, pp. 84–94, 2017.

[43] S. G. Prolongo, M. R. Gude, and A. Ureña, "Water uptake of epoxy composites reinforced with carbon nanofillers," *Composites Part A: Applied Science and Manufacturing*, vol. 43, no. 12, pp. 2169–2175, 2012.

[44] I. A. Mir and D. Kumar, "Carbon nanotube-filled conductive adhesives for electronic applications," *Nanoscience Methods*, vol. 1, no. 1, pp. 183–193, 2012.

[45] J. Zhou and J. P. Lucas, "The effects of a water environment on anomalous absorption behavior in graphite/epoxy composites," *Composites Science and Technology*, vol. 53, no. 1, pp. 57–64, 1995.

[46] M. Shettar, A. Chaudhary, Z. Hussain, U. A. Kini, and S. Sharma, "Hygrothermal studies on GFRP composites: A review," *Materials Science, Engineering and Chemistry (MATEC) Web Conf.*, vol. 144, pp. 1–9, 2018.

[47] C. Fromonteil, P. Bardelle, and F. Cansell, "Hydrolysis and oxidation of an epoxy resin in sub- and supercritical water," *Industrial & Engineering Chemistry Research*, vol. 39, no. 4, pp. 922–925, 2000.

[48] G. Z. Xiao and M. E. R. Shanahan, "Irreversible effects of hygrothermal aging on DGEBA/DDA epoxy resin," *Journal of Applied Polymer Science*, vol. 69, no. 2, pp. 363–369, 1998.

[49] B. Yu, P. He, Z. Jiang, and J. Yang, "Interlaminar fracture properties of surface-treated Ti-CFRP hybrid composites under long-term hygrothermal conditions," *Composites Part A: Applied Science and Manufacturing*, vol. 96, pp. 9–17, 2017.

[50] E. Greenhalgh, "Delamination-dominated failures in polymer composites," in *Failure Analysis and Fractography of Polymer Composites*, pp. 164–237, 2009.

[51] E. Greenhalgh, "Defects and damage and their role in the failure of polymer composites," in *Failure Analysis and Fractography of Polymer Composites*, pp. 356–440, 2009.

[52] G. Xiao, E. Liu, T. Jin, X. Shu, Z. Wang, G. Yuan, and X. Yang, "Mechanical properties of cured isotropic conductive adhesive (ICA) under hygrothermal aging investigated by micro-indentation," *International Journal of Solids and Structures*, vol. 122–123, pp. 81–90, 2017.

[53] S. Jasmee, G. Omar, S. S. C. Othaman, N. A. Masripan, and H. A. Hamid, "Interface thermal resistance and thermal conductivity of polymer composites at different types, shapes, and sizes of fillers: A review," *Polymer Composites*, vol. 42, no. 6, pp. 2629–2652, 2021.

[54] F. M. Coughlan and H. J. Lewis, "A study of electrically conductive adhesives as a manufacturing solder alternative," *Journal of Electronic Materials*, vol. 35, no. 5, pp. 912–921, 2006.

[55] P. M. Brogly and P. Polyme, "Forces involved in adhesion," in *Handbook of Adhesion Technology*, pp. 40–63, 2011.

[56] Y. Niu, Y. Yan, and J. Yao, "Hygrothermal aging mechanism of carbon fiber/epoxy resin composites based on quantitative characterization of interface structure," *Polymer Testing*, vol. 94, pp. 1–6, 2021.